One-step purification of assembly-competent tubulin from diverse eukaryotic sources

Per O. Widlund*, Marija Podolski*, Simone Reber, Joshua Alper, Marko Storch, Anthony A. Hyman, Jonathon Howard, and David N. Drechsel
Max Planck Institute of Molecular Cell Biology and Genetics, 01307 Dresden, Germany

ABSTRACT **We have developed a protocol that allows rapid and efficient purification of native, active tubulin from a variety of species and tissue sources by affinity chromatography. The affinity matrix comprises a bacterially expressed, recombinant protein, the TOG1/2 domains from *Saccharomyces cerevisiae* Stu2, covalently coupled to a Sepharose support. The resin has a high capacity to specifically bind tubulin from clarified crude cell extracts, and, after washing, highly purified tubulin can be eluted under mild conditions. The eluted tubulin is fully functional and can be efficiently assembled into microtubules. The method eliminates the need to use heterologous systems for the study of microtubule-associated proteins and motor proteins, which has been a major issue in microtubule-related research.**

Monitoring Editor
David G. Drubin
University of California, Berkeley

Received: Jun 12, 2012
Revised: Sep 12, 2012
Accepted: Sep 13, 2012

INTRODUCTION

Tubulin is the major building block of microtubules (Snyder and McIntosh, 1976; Desai and Mitchison, 1997; Howard and Hyman, 2003), the cytoskeletal polymer present in all eukaryotic organisms and used for critical cellular processes such as intracellular transport and chromosome segregation. Consistent with their roles in chromosome segregation and cell division, microtubules are targeted by a number of anticancer drugs in the taxane and vinca alkaloid family (Schiff *et al.*, 1979). Furthermore, microtubules associate with a large number of motors and microtubule-associated proteins (Akhmanova and Steinmetz, 2008). These interactions have been the subject of intense biochemical studies over the past 40 yr (Kirkpatrick *et al.*, 1970; Murphy and Borisy, 1975).

In vitro studies of tubulin and associated proteins have been critical to elucidate their roles in cells. For these types of studies, it is often necessary to purify large amounts of tubulin. However, purification of native, untagged tubulin from most sources has proved difficult because tubulin is not abundant in most cell and tissue types. At present, it is most efficient to purify tubulin from either porcine or bovine brains. Brains have a sufficiently high concentration of tubulin to permit microtubule assembly in crude extracts and subsequent fractionation of polymerized microtubules by sedimentation. These protocols rely on tubulin's reversible, temperature-sensitive polymerization properties (Weisenberg, 1972). Brain homogenates are taken through rounds of "cycling" in which where microtubules are assembled, pelleted, and disassembled to eventually yield large amounts of pure tubulin after removal of associated proteins by phosphocellulose chromatography (Weingarten *et al.*, 1975). This purified brain tubulin readily assembles into microtubules in vitro. Much of what is known about microtubule dynamics (Desai and Mitchison, 1997), regulation of their assembly (Howard and Hyman, 2007), and their interaction with associated proteins (Mandelkow and Mandelkow, 1995), as well as about the motility of motor proteins (McIntosh and Pfarr, 1991), has been learned by studying brain tubulin.

There are a number of drawbacks to using tubulin from mammalian brain. The first is that, when studying motors or microtubule-associated proteins from other organisms, the native tubulin is not used. Although tubulin is conserved in eukaryotes, interactions are likely to be affected when heterologous components are used in reconstituted biochemical assays (Alonso *et al.*, 2007). Furthermore, brain tubulin has a unique and complex mixture of different isotypes (i.e., tubulin expressed from different genes) and isoforms (i.e., tubulins with different posttranslational modifications) that is not representative of most other cell types (Villasante *et al.*, 1986; Panda *et al.*, 1994; Luduena, 1998; Janke and Bulinski, 2011).

This article was published online ahead of print in MBoC in Press (http://www.molbiolcell.org/cgi/doi/10.1091/mbc.E12-06-0444) on September 19, 2012.

*These authors contributed equally to this work.

Address correspondence to: David N. Drechsel (drechsel@mpi-cbg.de).

Abbreviations used: CV, column volume; GST, glutathione *S*-transferase; MAPs, microtubule-associated proteins; NHS, N-hydroxysuccinimide ester.

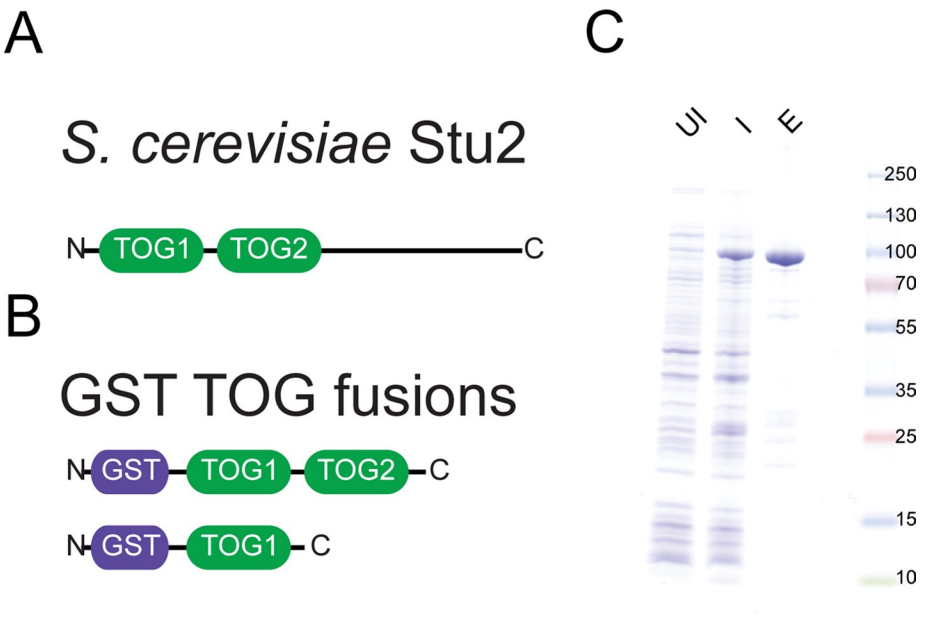

FIGURE 1: The purification matrix. (A) The domain structure of *S. cerevisiae* Stu2 (YLR045C) protein. TOG1 spans residues 8–280, and TOG2 spans residues 326–550. (B) GST-TOG fusion constructs used in this study. (C) Expression and purification of the GST-TOG1/2 fusion protein after overexpression in *E. coli*. Lanes: Total cell extract before induction (UI) and after induction (I) and the glutathione elute (E).

Purification of tubulin from sources other than mammalian brain has only been successful in a limited number of systems (Kuriyama, 1976; Binder and Rosenbaum, 1978; Kilmartin, 1981; Dawson *et al.*, 1983; Suprenant and Rebhun, 1984; Barnes *et al.*, 1992; Drummond *et al.*, 2011). Significantly, the expression of polymerization-competent recombinant eukaryotic tubulin in bacteria has been unsuccessful. Coexpression of tagged tubulin with native isoforms in *Saccharomyces cerevisiae* is possible (Johnson *et al.*, 2011), but the tagged form cannot fully substitute for the function of the native α/β-tubulin. Tagging, therefore, appears to interfere with biological function. Here we describe a method, based on affinity chromatography, that allows rapid and efficient purification of native, active tubulin from diverse species or tissue sources.

RESULTS

Purification matrix

We developed a simple one-step method to purify tubulin from diverse eukaryotic sources. The method takes advantage of the XMAP215/Dis1 family of microtubule-associated proteins (MAPs; Gard and Kirschner, 1987; Gard *et al.*, 2004). Specifically, it exploits what is believed to be the physiological role of the conserved N-terminal TOG domains. In cells, XMAP/Dis proteins, residing at microtubule ends, catalyze assembly of subunits onto the growing tip by the selective binding and release of tubulin dimers recruited from the cytoplasmic pool (Al-Bassam *et al.*, 2006, 2007; Brouhard *et al.*, 2008; Widlund *et al.*, 2011). These binding properties render the TOG domain ideal for affinity purification because tubulin is selectively bound from cytoplasmic extracts, but perhaps more important, it is readily released such that it remains in an active state. We fused either the first or both TOG domains of the *S. cerevisiae* protein Stu2 to glutathione *S*-transferase (GST; Figure 1, A and B) and expressed these fusion proteins in *Escherichia coli*. The GST-TOG1 or GST-TOG1/2 fusion was then purified on a glutathione Sepharose column (Figure 1C), desalted, and conjugated to an N-hydroxysuccinimide ester–activated Sepharose column (NHS column) to prepare what we call a TOG1 or TOG1/2 column.

Purification and assembly of *Spodoptera frugiperda* tubulin

As proof of principle, tubulin was first purified from cultured *S. frugiperda* (SF+) cells. We prepared extracts from these cells in a standard microtubule assembly buffer (80 mM 1,4-piperazinediethanesulfonic acid, 1 mM MgCl2, 1 mM ethylene glycol tetraacetic acid [EGTA], pH 6.8; BRB80 buffer) and after clarification loaded this extract onto a TOG1/2 column that had been equilibrated with BRB80. The column was washed with BRB80 containing GTP, ATP, Tween 20, and 10% glycerol and was then eluted with BRB80 adjusted to high ionic strength. The eluted protein was then promptly desalted, concentrated, and, after addition of glycerol, flash frozen in liquid nitrogen (Figure 2A). The eluted protein migrated as a closely space doublet at 50 kDa in SDS–PAGE gel. The identification of this doublet, present in the eluate, as α/β-tubulin and its level of depletion by the affinity matrix were assessed by Western blot using a pan-specific anti–α-tubulin monoclonal antibody (Figure 2B). The Western blot confirmed that one band from this doublet represents α-tubulin. Quantification of the level of depletion by Western blotting reveals that at least 95% of the α-tubulin present in the clarified lysate is bound by the resin (Figure 2B). These results show that the TOG1/2 column is highly selective and efficient for isolating tubulin from crude cell extracts.

We tested whether the final preparation after affinity purification remained assembly competent, because purified tubulin is highly labile. Purified insect tubulin was induced to polymerize in BRB80 buffer by adding glycerol and GTP. The mixture was incubated at 25°C for 30 min. Polymer and monomer pools were separated by sedimentation and the levels of protein present in these fractions compared by SDS–PAGE. At least 70% of the total tubulin was found in the pelleted polymer fraction after the assembly reaction (Figure 2C), suggesting that the bulk of the tubulin present was assembly competent.

The sedimentation assay cannot distinguish between tubulin assembled into microtubules or into other polymeric forms such as sheets, ribbons, rings, or even aggregates of denatured tubulin. To find out whether the affinity-purified tubulin formed microtubules, samples of the polymerization reaction were imaged by electron microscopy. In negatively stained preparations, abundant long, 25-nm-wide polymers can clearly be seen (Figure 2D), showing that the pure *S. frugiperda* tubulin is assembly competent.

Purification of diverse tubulins

A diverse set of eukaryotic cells was selected to test whether this affinity purification protocol is broadly applicable. Extracts of human embryonic kidney (HEK293) cells, whole *Caenorhabditis elegans* worms, *S. cerevisiae*, *Xenopus laevis* eggs, and *Chlamydomonas reinhardtii* flagella were prepared. The tubulin was purified using TOG1/2 columns from cell extracts under conditions similar to those used for *S. frugiperda* except in the case of *S. cerevisiae*, for which

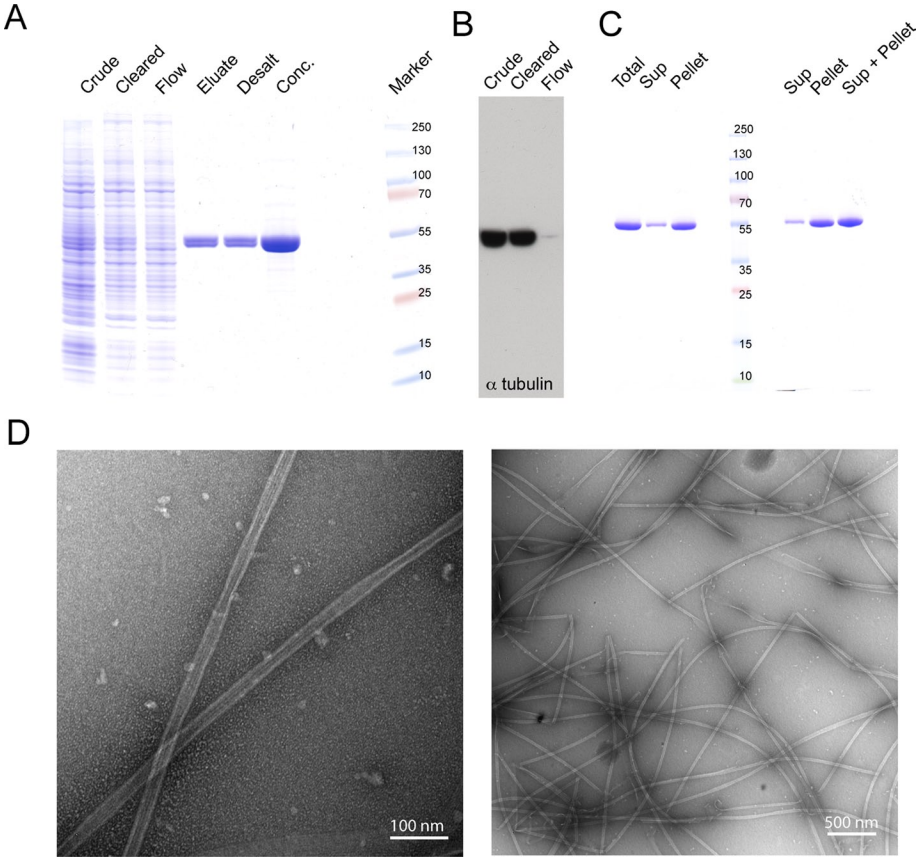

FIGURE 2: Purification of *S. frugiperda* (SF+) tubulin. (A) Samples throughout the purification were analyzed by SDS–PAGE and stained with Coomassie blue. The lanes are as follows: crude extract (Crude), high-speed extract (Cleared), TOG column flow through (Flow), eluate, desalted eluate, concentrated eluate (conc.). (B) The crude extract, cleared extract, and TOG column flowthrough were transferred to nitrocellulose and probed with DM1 α-tubulin antibody. Tubulin in the extract was >95% depleted by a single pass over the TOG column. (C) Polymerization and sedimentation of SF+ tubulin. Tubulin was polymerized in the presence of GTP and glycerol and the monomer and polymer pools separated by sedimentation over glycerol cushions. Left lanes, total assembly reaction (Total), supernatant (Sup), and pellet. Right lanes, supernatant (Sup), pellet, and combined supernatant and pellet. (D) SF+ tubulin was polymerized in GTP and glycerol, stabilized with Taxol, deposited on formvar-coated grids, and negatively stained. Images are at 39,000× and 6600× magnification.

the TOG1 column was used. In each case, tubulin was bound and efficiently eluted to yield preparations of equivalent purity (Figure 3). The extracts from frog eggs and whole worms were also depleted to a similar level compared with SF+ (Figure 4A). Yields for the various purifications are shown in Table 1, with the exception of *C. reinhardtii,* for which a substantial portion of the tubulin passed through the TOG1/2 column unbound (Figure 3F). In this last case, the unbound fraction may represent tubulin oligomers or tubulin that became denatured during disassembly of the stable flagellar microtubules. In addition, we determined what proportion of the loaded tubulin was retained by the TOG1/2 resin after elution with high ionic strength. Less than 1% of the loaded porcine tubulin remained tightly associated, suggesting that there is not a class of tubulin that is of particularly high affinity (Figure 4B).

All of these diverse tubulins appeared polymerization competent (Figure 5). As shown in electron micrographs, *C. elegans* and *X. laevis* tubulin assembled into 25-nm filaments. Using in vitro assembly and sedimentation to separate microtubules from unassembled polymer, human tubulin prepared from HEK cells was shown to polymerize efficiently. Finally, *S. cerevisiae* tubulin showed dynamic assembly of microtubules by differential interference contrast (DIC) microscopy (Supplemental Movie S1).

Whereas tubulin purified from SF+ cells showed very low levels of copurifying proteins, initial preparations of tubulin from other species yielded more prominent contaminating bands (Figure 6A). The most prominent bands in both the *C. elegans* and *X. laevis* preparations were excised from gels, digested, and identified by mass spectrometry (Table 2). Of interest, for both species, the chaperone proteins Hsp90, Hsp70, Sti1 (Hop), and Hsp40 copurified with tubulin. An additional Sti1-like protein also copurified with *C. elegans* tubulin. Aldolase copurified with *Xenopus* tubulin, an interaction that was previously detected (Karkhoff-Schweizer and Knull, 1987). The presence of the chaperones in our purifications prompted us to include an ATP wash step in order to effect release from their target. Indeed, when this step was included in the purification protocol for *C. elegans* tubulin, the copurifying bands were significantly reduced (Figure 6B).

DISCUSSION

Most mechanistic studies of MAPs and motor proteins from model organisms used heterologous systems with microtubules assembled from bovine or porcine brain tubulin because it has been difficult to isolate sufficient amounts of active tubulin from most species. This use of heterologous systems may confound interpretation of these mechanistic studies because the dynamic properties of microtubules, as well as their interaction with motors, vary considerably, depending on the source of tubulin (Detrich *et al.*, 2000; Newton *et al.*, 2002; Bode *et al.*, 2003; Alonso *et al.*, 2007; Erent *et al.*, 2012). We provide a widely accessible method to eliminate this major problem in tubulin and microtubule-related research. The TOG domains of *S. cerevisiae* Stu2 bind to every tubulin we tested from a diverse set of eukaryotes. If exceptions exist, it is likely that a fragment of the TOG protein from that species will work in a similar way. TOG proteins have been found in all eukaryotes examined (Gard *et al.*, 2004; Al-Bassam and Chang, 2011).

A major advantage of this method is its efficiency. In mammalian brain extracts, tubulin was found to account for at least 20% of the soluble protein (Hiller and Weber, 1978). Owing to this high concentration, tubulin readily polymerizes in crude extracts, and the assembled microtubules readily fractionate away from the bulk cytoplasmic protein by sedimentation. However, most other cell types and tissues express much less tubulin, which makes such a polymerization and sedimentation strategy a less efficient purification step from crude extracts. Extracts from cultured cells, such as 3T3, contain only 3% tubulin (Hiller and Weber, 1978), and *S. cerevisiae* extracts reportedly contain only 0.05% tubulin (Kilmartin, 1981) However, even at these low concentrations, the TOG column was able to efficiently fractionate tubulin to a high purity. We calculated

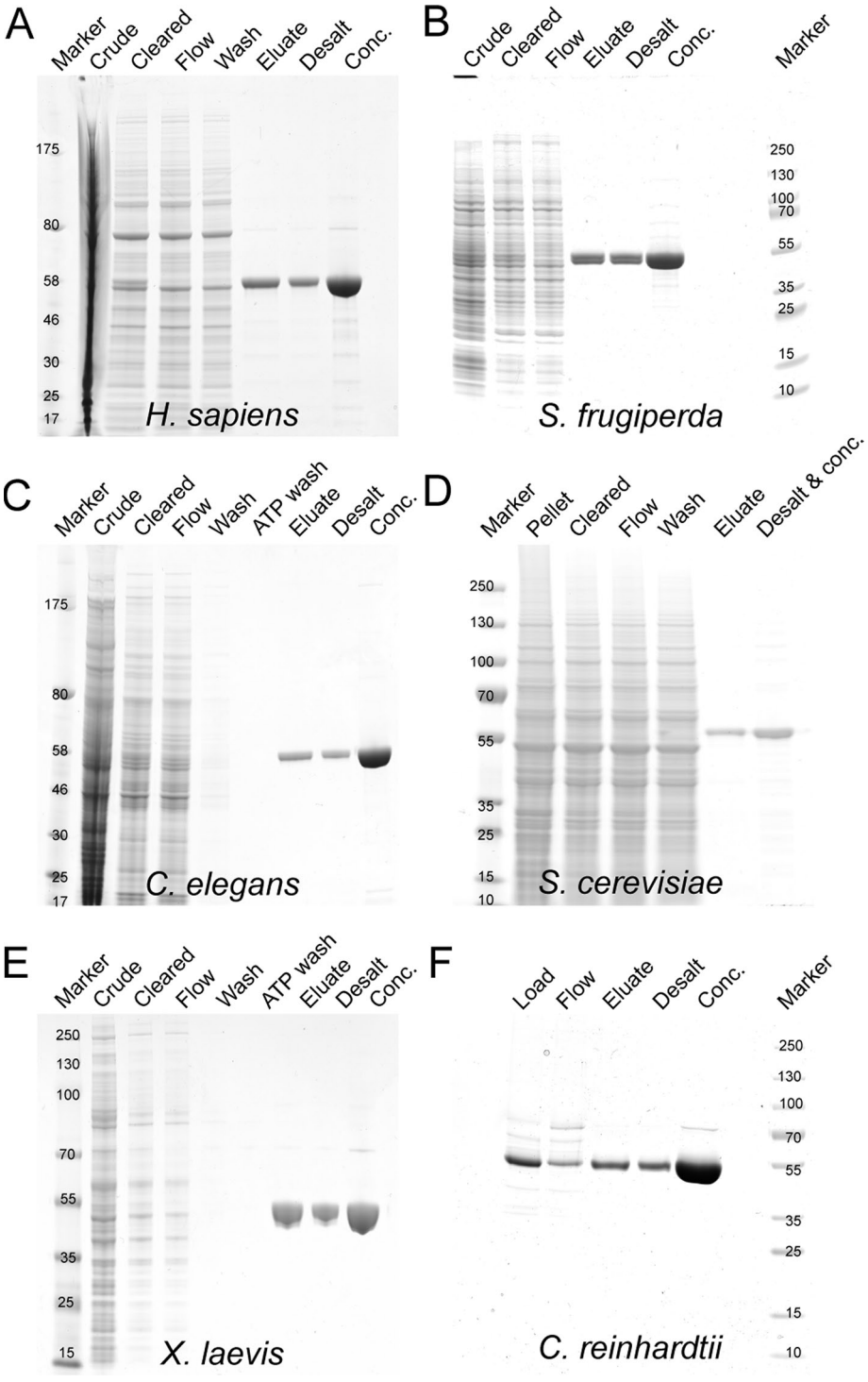

FIGURE 3: Purification of tubulins from various species and tissue types. Samples collected throughout each purification were analyzed by SDS–PAGE and stained with Coomassie blue. (A) *H. sapiens* HEK293 cells. (B) *S. frugiperda* SF+ cells. (C) *C. elegans* whole N2 worms. (D) *S. cerevisiae* cells. (E) *X. laevis* eggs. (F) *C. reinhardtii* flagella.

the yield of purified tubulin from each of our purifications (Table 1). Tubulin could be eluted from a 1-ml TOG column at concentrations of up to 1.4 mg/ml, with a total yield of up to 3.5 mg, the apparent saturation point of our 1-ml column. We also calculated the yield of tubulin per milligram of total protein in our extracts. The yields met or exceeded the published values for the abundance of tubulin in cell extracts. Although we do not directly measure the amount of tubulin present in the crude cell lysates, these high yields, as well as the efficient removal of tubulin from the unbound fraction during affinity chromatography, support our conclusion that most of the available tubulin present in the extracts is efficiently bound and retained by the TOG column.

The tubulin eluted from the TOG column is nearly pure in a single affinity step. However, in the absence of an ATP wash step, a number of proteins copurify with tubulin. The majority of these proteins belong to the class of protein chaperones. Although these chaperone proteins can form a complex (Ran *et al.*, 2008), we cannot conclude from our data whether they bind directly to tubulin, either individually or as a complex, or if they simply bind to the TOG1/2 affinity matrix. Future studies are needed to distinguish these possibilities. However, genetic and biochemical evidence suggests that the interaction between tubulin and heat shock proteins is physiologically relevant (Weis *et al.*, 2010; Silflow *et al.*, 2011).

The cycling tubulin protocols result in substantial tubulin losses at each step. We estimate that only ~1% of the total tubulin originally present in brain is recovered in purified form from a typical large-scale cycling preparation. This is not only inefficient, but also it is potentially highly selective for certain isotypes and isoforms of tubulin. Based on quantification of tubulin levels from Western blots, the TOG column generally recovered >95% of the soluble tubulin from any extract, suggesting that TOG domains do not bind preferentially to certain isotypes or isoforms of tubulin. Furthermore, <1% of porcine brain tubulin was retained by TOG1/2 resin after elution with high ionic strength. This small fraction likely represents nonspecific adsorption, perhaps due to tubulin denaturation during chromatography. Therefore, the tubulin pool that elutes is likely to be representative of that particular cell type. Consequently, our method may be useful for comparative studies of different tissue and cell types because the purified tubulin may assemble into microtubules that have properties required for that particular tissue or cell type.

MATERIALS AND METHODS

Expression and purification of TOG domains

Gene fragments encoding the first (residues 1–306) and both (residues 1–590) of the tandem N-terminal TOG domains found in *S. cerevisiae* Stu2 were subcloned into pGEX-6P-1 for expression of GST fusions in *E. coli* (pGEX-6P-1 Stu2 1-306; pGEX-6P-1 Stu2 1-590). Fresh transformants of the expression plasmids in BL21(DE3) T1 pRARE were used to inoculate an overnight culture in MDAG-135 medium (Studier, 2005) containing antibiotics (100 µg/ml

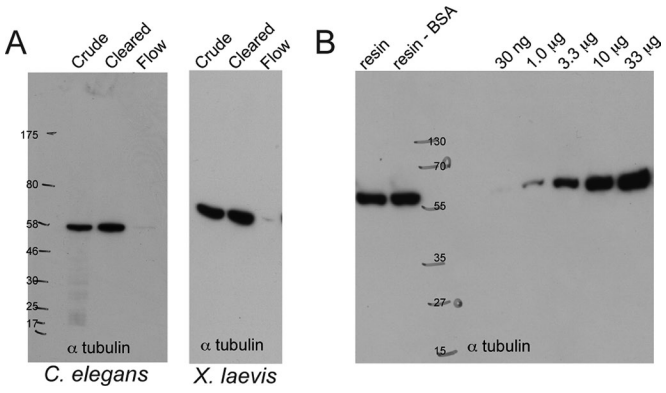

FIGURE 4: Efficiency of tubulin depletion and elution. (A) Tubulin was detected in samples taken from the crude extract, cleared crude extract, and the TOG column flowthrough by Western blotting using an α-tubulin antibody: depletion of *C. elegans* extracts (98%), depletion of *X. laevis* extracts (94%). (B) A 100-µl amount of TOG1/2 resin was incubated either with bovine serum albumin or buffer, followed by 1 mg of porcine tubulin. The resin was then washed with buffers used in a standard SF+ tubulin purification and then boiled in SDS–PAGE sample buffer. These two samples along with known amounts of porcine tubulin were run on SDS–PAGE and analyzed on Western blots using an α-tubulin antibody (DM1α).

ampicillin and 15 µg/ml chloramphenicol). This culture was diluted 500-fold into 1 l of Terrific Broth (1.2% tryptone, DIFCO 211705; 2.4% yeast extract, DIFCO 2212750; 0.4% glycerol; 17 mM KH_2PO_4; 72 mM K_2HPO_4) with the same antibiotics and shaken at 37°C until the OD_{600} reached 0.5. After shifting the cultures to 18°C for 1 h, expression was induced by adding 0.2 mM isopropyl β-D-1-thiogalactopyranoside and shaking for 18 h. Induced cultures were pelleted (5000 rpm, 10 min at 4°C, JLA 8.1000; Beckman Coulter, Brea, CA) and then resuspended in an equal volume of 2× phosphate-buffered saline (PBS) made from a 10× stock (10× PBS: 27 mM KCl, 15 mM KH_2PO_4, 81 mM Na_2HPO_4, 1.37 M NaCl) with 1 mM dithiothreitol (DTT). After addition of benzonase (Novagen, Gibbstown, NJ) and protease inhibitors, the cells were lysed using two passes through an ice-cold Emulsiflex C5 microfluidizer (Avestin, Ottawa, Canada) at 1500 bar. The lysate was clarified by two sequential centrifugation steps (12,000 rpm, 30 min at 4°C; Beckman JA-12) and then applied to a GSTrap (5 ml = 1 column volume [CV]; GE Healthcare, Buckinghamshire, United Kingdom) preequilibrated in 2× PBS with 1 mM DTT (wash buffer) at 0.5 CV/min. The column was then washed with 10 CV of wash buffer with 0.1% Tween 20 and then 2 CV of 5 mM ATP with 10 mM $MgCl_2$ in 2× PBS. The column was incubated for 20 min and then washed with 5 CV of 6× PBS, followed by 5 CV of wash buffer. The GST fusion was eluted using 5 mM reduced glutathione in wash buffer at pH 8.0. The pool of eluted protein was desalted or dialyzed against three changes of 100 mM $NaHCO_3$ with 100 mM NaCl at pH 8.2 (coupling buffer). The concentration of the GST fusion was determined by measuring the absorbance at 280 nm using a NanoDrop spectrophotometer (NanoDrop Technologies, Wilmington, DE) and the calculated extinction coefficient. One liter of bacterial culture yielded approximately 70 mg of GST-TOG1/2 fusion.

Preparation of the tubulin affinity resin

Tubulin affinity columns were prepared by coupling GST-TOG1/2 fusions to HiTrap NHS-activated HP columns (1 and 5 ml; GE Healthcare) following the manufacturer's instructions with modifications. Before coupling, 80 mM $MgCl_2$ was added to the dialyzed GST-fusion preparation in coupling buffer. Immediately after washing the HiTrap NHS-activated HP columns with 3 CV of ice-cold 1 mM HCl at 1.5 CV/min, coupling was performed by continuously recirculating the GST-TOG1/2 fusion (1.5 CV/min, 4 CV of a 4 mg/ml preparation) for 30 min at room temperature. Unreacted NHS groups were blocked by washing with 6 CV of 0.5 M ethanolamine and 0.5 M NaCl at pH 8.3 and then incubated for 30 min at room temperature. The column was then washed with 6× PBS, followed by 1× PBS with 50% glycerol (storage buffer) and stored at –20°C. The coupling efficiency was >75% as assessed by comparing protein levels on SDS–PAGE before and after incubation with the resin, meaning that at least 12 mg of GST-TOG12 fusion was coupled to a 1-ml column. The columns retained the capacity to bind tubulin for at least 4 mo when stored at –20°C and could be used repetitively if washed between runs with 10 CV of 10× PBS, followed by 5 CV of 1× PBS and then 5 CV of storage buffer.

Purification using the TOG affinity column

The protocol for SF+ extracts was developed most extensively. The only notable differences between this primary example and the purifications from other later sources, described later, are in the wash and elution steps. Although GTP, Tween 20, and glycerol were not uniformly included in subsequent purifications, these additives may improve the purity and assembly properties of the tubulins purified with the following methods. The inclusion of Tween 20 and glycerol during wash steps improved the quality of our eluted SF+ tubulin preparation, as judged from electron micrographs of microtubules. Similarly, the substitution of ammonium sulfate for potassium chloride in the elution buffer, based on an earlier report in which this salt was shown to reduce loss of bound nucleotide, may improve the assembly properties of the final preparations (Croom *et al.*, 1986). In all the preparations, one should take care to limit the length of exposure of tubulin to high salt by rapidly desalting into storage buffer (e.g., BRB80).

	Cell pellet (g)	Total protein loaded (mg)	Eluted [tubulin] (mg/ml)	Total tubulin yield (mg)	[Tubulin] after ultrafiltration (mg/ml)	Tubulin yield/protein loaded (%)
X. laevis	4.0	32.7	1.0	2.5	3.4	7.6
H. sapiens	7.5	69.3	1.4	3.5	2.0	5.0
S. frugiperda	2.1	17.5	0.7	1.9	2.9	10.7
C. elegans	4.0	16.8	0.2	0.4	2.0	2.4
S. cerevisiae	66.0	89.0	0.04	0.1	0.7	0.1

The columns are, left to right: weight of the cell pellet, total protein present in the clarified extract, initial concentration of the eluted tubulin, total yield of tubulin, the final tubulin concentration after ultrafiltration, and the yield of purified tubulin as the percentage of total protein in the clarified extract.

TABLE 1: Purification yields.

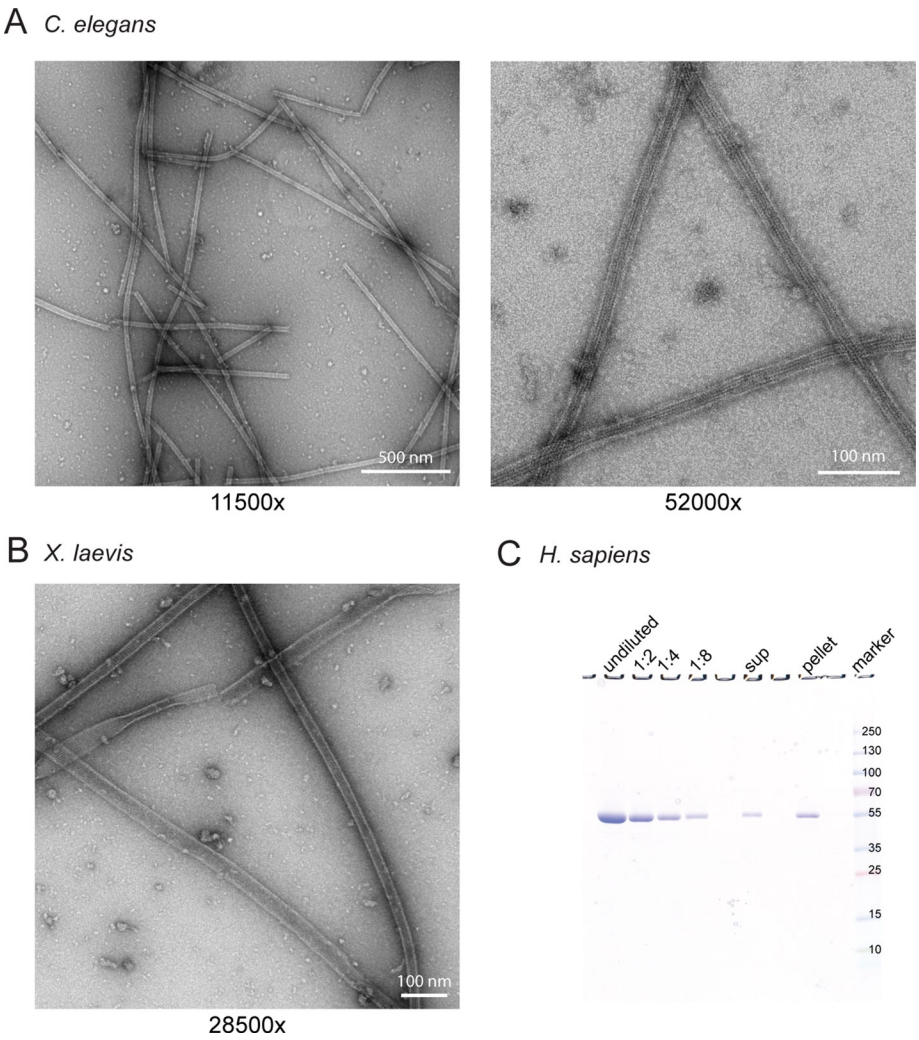

FIGURE 5: Polymerization competence of tubulins. Electron micrographs of microtubules polymerized from *C. elegans* (A) and *X. laevis* (B) tubulin. Tubulins were polymerized in GTP and glycerol, stabilized with Taxol, and then deposited on formvar-coated grids and negatively stained. (C) Human tubulin was polymerized in the presence of GTP and glycerol and the monomer and polymer pools separated by sedimentation over glycerol cushions. Left four lanes, serial dilutions of the total assembly reaction; middle lane, supernatant (Sup); right lane, pellet.

Purification of *S. frugiperda* tubulin

SF+ cells (500 ml) were grown to 4×10^6 cells/ml in SF900II medium (Invitrogen, Carlsbad, CA) and pelleted by centrifugation at 1700 × *g* for 15 min. Cells were resuspended in an equal volume of 1× BRB80 containing 3 U of benzonase, 1 mM DTT, and protease inhibitors. Cells were lysed by douncing on ice (20 strokes). The extract was cleared by centrifugation (80,000 rpm, 10 min, 4°C, Sorvall S100 AT6; Sorvall-Hitachi, Thermo Scientific, Waltham, MA) and then filtered through a 0.45-µm Milliex-HV polyvinylidene fluoride membrane (Millipore, Bedford, MA). The purification was performed at 4°C. The extract was loaded at 0.5 CV/min onto a TOG column pre-equilibrated with 1× BRB80 and followed by 4 CV of 1× BRB80 and 100 µM Mg^{2+} GTP to clear out most of the extract from the column. The flow rate was then changed to 1 CV/min for the following wash steps: 1) 10 CV of 1× BRB80, 10 µM Mg^{2+} GTP; 2) 3 CV of 1× BRB80, 100 µM Mg^{2+} GTP, 10 mM $MgCl_2$, and 5 mM ATP followed by a 15-min incubation; 3) 5 CV of 1× BRB80 and 10 µM Mg^{2+} GTP; and 4) 5 CV of 1× BRB80, 0.1% Tween 20 and 10% glycerol. The tubulin was eluted with 3 CV of 1× BRB80, 10 µM Mg^{2+} GTP, and 500 mM $(NH_4)_2SO_4$. Ammonium sulfate was used because tubulin has been shown to better retain its nucleotide in the presence of this salt (Croom *et al.*, 1986). After pooling, the amount of tubulin in the peak fractions was determined by Bradford assay (Bio-Rad, Richmond, CA). Care was taken to limit exposure of the tubulin to high salt. The eluate was quickly desalted into 1× BRB80 and 10 µM Mg^{2+} GTP with a PD10 desalting column. GTP can be omitted or used at lower concentration for subsequent assembly with alternative nucleotides like GMPCPP. The tubulin was concentrated to at least 20 µM with an Amicon Ultra 10K MWCO centrifugal filter (Millipore), and glycerol was added to 5% before snap freezing in liquid nitrogen. The column was then washed with 10× PBS and could then either be reequilibrated or stored in 50% glycerol and 1× PBS at –20°C.

Purification of *Homo sapiens* HEK293 tubulin

A 500-ml culture at 2×10^6 cells/ml in FreeStyle 293 medium was harvested by centrifugation at 1700 × *g* for 15 min. The tubulin purification was performed as per the SF+ protocol except that the Tween/glycerol wash step was omitted.

Purification of *C. elegans* tubulin

Worms were cultured using a modified protocol from that found in the WormBook (Stiernagle, 2006). A preculture of C600 bacteria was used to inoculate 1 l of Luria–Bertani medium (1% tryptone, DIFCO 211705; 0.5% yeast extract, DIFCO 2212750; 171 mM NaCl, pH 7.0) medium and incubated overnight at 37°C. The bacteria were pelleted at 5000 relative centrifugal force (rcf) in sterilized centrifuge bottles, resuspended in 10 ml S-Basal (0.02 M K_2HPO_4, 0.043 M KH_2PO_4, 0.1 M NaCl, 4 mg/l cholesterol), and transferred to 50-ml Falcon tubes (Fisher Scientific, Pittsburgh, PA). The resuspended pellet was stored at –80°C.

Nine large (8 cm) OP50/NGM plates were seeded with 15 adult hermaphrodites (N2) each. The worms were allowed to grow until starved and then collected into Falcon tubes from plates using S complete medium supplemented with penicillin, streptomycin, and nystatin. The worms were washed twice with the same medium. The suspension was then used to inoculate 2× 1 l of liquid culture consisting of S complete medium supplemented with nystatin. The worms were grown at 22°C with vigorous shaking to ensure sufficient oxygen supply (~200 rpm) for 2–3 d. More bacteria were added if growth slowed during this time. The worms were harvested by letting them settle 4 h at 4°C. Media was decanted, and worms were transferred to a 50-ml Falcon tube and then washed twice with cold M9 medium. As much media as possible was removed before storing the worms at –80°C. The worm pellet was resuspended in an equal volume of 1× BRB80 supplemented with protease inhibitor cocktail (Roche, Indianapolis, IN). The slurry was frozen dropwise in

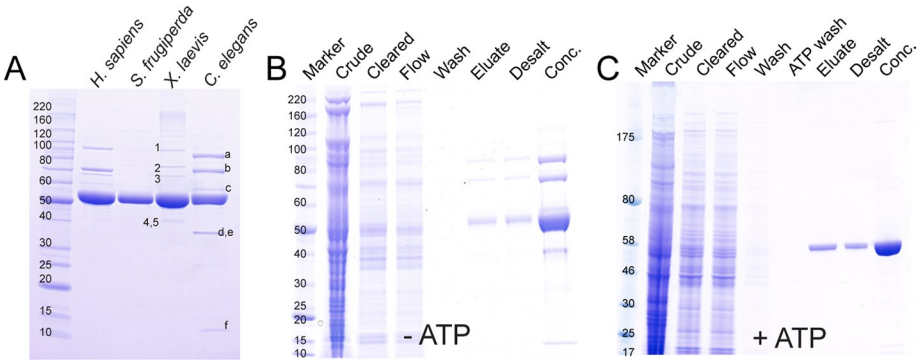

FIGURE 6: Identification and removal of proteins copurifying with tubulin. (A) A Coomassie blue–stained gel with tubulins purified from HEK293, SF+, frog egg extracts, and whole worms. Mass spectrometry was used to identify the labeled bands: (1) Hsp90 (83 kDa), (2) Hsp70 (71 kDa), (3) Sti1 (62 kDa), (4) Aldolase (39 kDa), (5) Hsp40 (38 kDa). (a) Hsp90 (80 kDa), (b) Hsp70 (70 kDa), (c) Sti1-like (45 kDa), (d) Sti1 (37 kDa), (e) Hsp40 (36 kDa), (f) ZK856.7 (13 kDa). (B, C) Purification of *C. elegans* tubulin without (B) and with (C) an ATP wash step. Samples taken throughout the purification were run on SDS–PAGE and stained with Coomassie blue.

liquid nitrogen and ground to a powder with a mortar and pestle under liquid nitrogen and then allowed to thaw on ice. The tubulin purification was performed as per the SF+ protocol, except that the Tween/glycerol wash step was omitted.

Purification of *S. cerevisiae* tubulin

For purification of budding yeast tubulin, we used strain BY4741 (Brachmann *et al.*, 1998; Mat a, his3Δ1, leu2Δ0, met15Δ0, ura3Δ0). Nine liters of culture was grown at 30°C with shaking at 180 rpm until OD_{600} of 1.5. Cells were pelleted and washed in doubly distilled H_2O, and pellets were ground in liquid nitrogen as previously described (Sorger *et al.*, 1988). Lysate powder was stored at –80°C and thawed in lysis buffer before use (3 ml of lysis buffer was added to 1 g of lysate powder). Lysis buffer consisted of BRB80, 10% glycerol, and 0.2% Triton X-100 supplemented with 5 μg /ml DNase I, 1 mM DTT, 0.1 mM ATP, 1 mM GTP, 0.2 mM phenylmethylsulfonyl fluoride, 5 μg/ml leupeptin, 1 μg/ml pepstatin A, and 1 μg/ml aprotinin. The lysate was stirred at 4°C for 10 min and sonicated using a Branson digital sonifier model 450D with 1/8-inch tapered microtip (Branson, Danbury, CT) set at 50% amplitude in 5× 10-s intervals with pauses of 30 s between pulses. The lysate was then centrifuged at 235,000 × *g*, 4°C for 30 min. Fresh PMSF was added to the supernatant to 0.2 μg/ml.

The supernatant was passed through a TOG1 column preequilibrated with lysis buffer at 0.5 ml/min. The column was washed with BRB80 and eluted with BRB80 with 500 mM KCl. Peak fractions were determined by Bradford assay and pooled. Pooled eluates were desalted into BRB80 and concentrated using an Amicon Ultra-4 10K centrifugal filter device (Millipore). Glycerol was added to 10% before the tubulin was aliquoted, snap frozen in liquid nitrogen, and stored at –80°C.

Protein ID	Gene name	Predicted molecular weight (kDa)
X. laevis		
Hsp90	hsp90ab1	83
Hsp70	hspa8	71
Sti1	stip1	62
Aldolase A	aldoa	39
DnaJ (Hsp40)	dnajb1	38
C. elegans		
Hsp90	DAF-21	80
Hsp70	HSP-1	70
Sti1 like	HIP-1	45
Sti1	STI-1	37
Hsp40	DNJ-13	36
Unknown	ZK856.7	13

TABLE 2: Mass spectrometry IDs.

Purification of *X. laevis* egg tubulin

CSF-extract was prepared according to Murray (1991). The extract was then diluted with an equal volume of BRB80 and centrifuged at 80,000 rpm in an S100AT6-0123 rotor (Sorvall-Hitachi) for 10 min at 4°C. The tubulin purification was performed as per the SF+ protocol, except that the Tween/glycerol wash step was omitted.

Purification of *C. reinhardtii* flagellar tubulin

The *C. reinhardtii* cells (CC-2228 oda1 mt+) were grown in liquid Tris-acetate-phosphate medium (20 mM Tris HCl, 7 mM NH_4Cl, 0.40 mM $MgSO_4$, 0.34 mM $CaCl_2$, 2.5 mM Na_3PO_4, and 1000× diluted Hutner's trace elements (Gorman and Levine, 1965), titrated to pH 7.0 with glacial acetic acid) with continuous aeration and 24 h of light at room temperature. Cultures (60 l) were grown to ~5 × 10^6 cells/ml. Cells were harvested and the axonemes were isolated by standard methods (Witman, 1986). Briefly, cells were harvested by centrifugation (800 × *g* for 7 min). They were deflagellated by 1.5 min of exposure to 4.2 mM dibucane-HCl. The deflagellation was quenched by 2× dilution and the addition of 0.5 mM EGTA. The flagella were separated from the cell bodies by centrifugation (1100 × *g* for 7 min and 1100 rcf for 20 min on a 30% sucrose cushion). The collected flagella were concentrated by resuspending the pellet after centrifugation (28,000 rcf) in 10 ml of HMDE (30 mM 4-(2-hydroxyethyl)-1-piperazineethanesulfonic acid, 5 mM $MgSO_4$, 1 mM DTT, and 1 mM EGTA titrated to pH 7.4 with KOH) with 0.4 μM Pefabloc (Sigma-Aldrich, St. Louis, MO). The flagella were demembranated by the addition of 0.2% IGEPAL CA-630 (Sigma-Aldrich), and then they were washed in HMDE. The axonemes were stripped of many microtubule-associated proteins with 20 min of incubation in HMDE plus 0.6 M KCl. After centrifugation (45,000 × *g*), the pellet was resuspended in HMDE plus 50 mM $CaCl_2$. It was sonicated for 10× 1-min-on/1-min-off cycles in an ice-cold sonicating bath to induce the axonemal microtubules to depolymerize. It was then centrifuged at 45,000 × *g* for 10 min. The supernatant was diluted fivefold in HMDE to reduce the $CaCl_2$ concentration.

The tubulin purification was performed as per the SF+ protocol, except that 1) the Tween/glycerol wash step was omitted, 2) GTP was not included in the purification, and 3) the tubulin was eluted in 1× BRB80 containing 0.5 M KCl. The *Chlamydomonas* tubulin was diluted to 10 μM in BRB80, flash frozen, and stored at –80°C.

Determination of protein

The level of tubulin in purified preparations was determined using the NanoDrop spectrophotomer and the estimated extinction coefficient for tubulin, 1.15 $(mg/ml)^{-1}$ cm^{-1}. Total protein in extracts was determined using either the Bradford assay or the bicinchoninic acid assay if buffers contained detergent.

Determination of tubulin depletion

Samples taken during the purification were resolved on SDS–PAGE and Western blotted using a pan-specific anti–α-tubulin monoclonal (DM1α) and a horseradish peroxidase–labeled secondary with enhanced chemiluminescence for detection. The level of tubulin was quantified using ImageJ software (Schneider *et al.*, 2012).

Determination of the elution efficiency

We loaded 1 mg of porcine brain tubulin onto 100 µl of TOG1/2 resin and then washed it and eluted the bound fraction under conditions similar to those described under purification of *S. frugiperda* tubulin. After the final high-salt elution, the resin was then boiled in SDS–PAGE sample buffer, and the amount of tubulin in this fraction was compared with known standards.

Negative-stain electron microscopy

Microtubules were polymerized in BRB80 containing 1 mM GTP for 30 min at 37°C. Microtubules were stabilized with 10 µM Taxol and then adsorbed for 2 min onto 200-mesh, glow-discharged, carbon-coated copper grids with formvar support (Electron Microscopy Sciences, Hatfield, PA). The samples were washed with 1× BRB80, stained in 50 µl of 2% uranyl acetate for 30 s, blotted, and air-dried. Grids were imaged on a CM100 transmission electron microscope (Philips/FEI Corporation, Eindhoven, Holland) operating at 80 kV. Micrographs were acquired using AMTV600 software operating an Advantage HS-B camera (2000 × 2000 pixels; AMT, Danvers, MA).

Mass spectrometry

Protein bands visualized by Coomassie staining were excised from the gel and their protein content digested with trypsin. The resulting peptide mixtures were extracted with 5% formic acid/50% acetonitrile and analyzed by liquid chromatography–tandem mass spectrometry on an Ultimate nanoLC system (Thermo Scientific Dionex, Amsterdam, Netherlands) interfaced online to a LTQ Orbitrap XL mass spectrometer (Thermo Fisher Scientific, Bremen, Germany) via a TriVersa robotic nanoflow ion source (Advion BioSciences, Ithaca NY) as described in Junqueira *et al.* (2008). Acquired spectra were searched against the National Center for Biotechnology Information protein database without species restriction using MASCOT software, version 2.2.0 (Matrix Science, London, United Kingdom), with the following settings: precursor mass tolerance was ±5 ppm; fragment mass tolerance was ±0.5 Da; variable modifications were propionamide (C), oxidation (M), and acetylation (protein N-terminus); enzyme was trypsin; two missed cleavages were allowed. Hits were evaluated using Scaffold software, version 2_04_00 (Proteome Software, Portland, OR), with the following settings: minimal number of matching peptides, two; peptide probability, 95%; protein probability, 99%; protein false discovery rate was calculated as 0.1%.

S. cerevisiae tubulin DIC imaging and assay conditions

Porcine brain tubulin was purified as described (Gell *et al.*, 2011) and labeled with TAMRA (Invitrogen; Hyman *et al.*, 1991). Rhodamine-labeled GMPCPP microtubules (25% labeled tubulin) were grown in BRB80 and 1 mM GMPCPP (Jena Bioscience, Jena, Germany), incubated for 2 h at 37°C, pelleted in an Airfuge (Beckman), and resuspended in BRB80. The flow cell assembly and preparation was performed as described (Varga *et al.*, 2006), with the exception that anti-rhodamine antibody was used. The objective was heated to 29°C. Yeast tubulin at 3 µM in BRB80 containing 1 mM GTP and antifade solution (40 mM glucose, 40 µg/ml glucose-oxidase, 16 µg/ml catalase, 0.1 mg/ml casein, 0.1% Tween 20, 1% DTT) was added to the chamber. Images were collected every 1.03 s for 11 min using the LED-VE-DIC setup described earlier (Bormuth *et al.*, 2007).

ACKNOWLEDGMENTS

We thank the Max Planck Institute of Molecular Cell Biology and Genetics (MPI-CBG) Electron Microscopy Facility for expertise, Anna Shevchenko and the MPI-CBG Mass Spectrometry Facility for analysis of tubulin purifications, Andy Hoenger and members of his lab for being gracious hosts, Linda Sandblad for technical expertise, Simon Alberti for providing the yeast strains, Anastasiya Trushko for help with the DIC experiment, Andrea Zinke for help with growing worms in culture, and Dick McIntosh for useful discussions.

REFERENCES

Akhmanova A, Steinmetz MO (2008). Tracking the ends: a dynamic protein network controls the fate of microtubule tips. Nat Rev. Mol Cell Biol 9, 309–322.

Al-Bassam J, Chang F (2011). Regulation of microtubule dynamics by TOG-domain proteins XMAP215/Dis1 and CLASP. Trends Cell Biol 21, 604–614.

Al-Bassam J, Larsen N, Hyman A, Harrison S (2007). Crystal structure of a TOG domain: conserved features of XMAP215/Dis1-family TOG domains and implications for tubulin binding. Structure 15, 355–362.

Al-Bassam J, van Breugel M, Harrison SC, Hyman A (2006). Stu2p binds tubulin and undergoes an open-to-closed conformational change. J Cell Biol 172, 1009–1022.

Alonso MC, Drummond DR, Kain S, Hoeng J, Amos L, Cross RA (2007). An ATP gate controls tubulin binding by the tethered head of kinesin-1. Science 316, 120–123.

Barnes G, Louie KA, Botstein D (1992). Yeast proteins associated with microtubules in vitro and in vivo. Mol Biol Cell 3, 29–47.

Binder LI, Rosenbaum JL (1978). The in vitro assembly of flagellar outer doublet tubulin. J Cell Biol 79, 500–515.

Bode CJ, Gupta ML, Suprenant KA, Himes RH (2003). The two alpha-tubulin isotypes in budding yeast have opposing effects on microtubule dynamics in vitro. EMBO Rep 4, 94–99.

Bormuth V, Howard J, Schaffer E (2007). LED illumination for video-enhanced DIC imaging of single microtubules. J Microsc 226, 1–5.

Brachmann CB, Davies A, Cost GJ, Caputo E, Li J, Hieter P, Boeke JD (1998). Designer deletion strains derived from *Saccharomyces cerevisiae* S288C: a useful set of strains and plasmids for PCR-mediated gene disruption and other applications. Yeast 14, 115–132.

Brouhard GJ, Stear JH, Noetzel TL, Al-Bassam J, Kinoshita K, Harrison SC, Howard J, Hyman AA (2008). XMAP215 is a processive microtubule polymerase. Cell 132, 79–88.

Croom HB, Correia JJ, Williams RC Jr (1986). The effects of elevated pH and high salt concentrations on tubulin. Arch Biochem Biophys 249, 397–406.

Dawson PJ, Gutteridge WE, Gull K (1983). Purification and characterisation of tubulin from the parasitic nematode, *Ascaridia galli*. Mol Biochem Parasitol 7, 267–277.

Desai A, Mitchison T (1997). Microtubule polymerization dynamics. Annu Rev Cell Dev Biol 13, 83–117.

Detrich HW 3rd, Parker SK, Williams RCJr, Nogales E, Downing KH (2000). Cold adaptation of microtubule assembly and dynamics. Structural interpretation of primary sequence changes present in the alpha- and beta-tubulins of Antarctic fishes. J Biol Chem 275, 37038–37047.

Drummond DR, Kain S, Newcombe A, Hoey C, Katsuki M, Cross RA (2011). Purification of tubulin from the fission yeast *Schizosaccharomyces pombe*. Methods Mol Biol 777, 29–55.

Erent M, Drummond DR, Cross RA (2012). S. pombe kinesins-8 promote both nucleation and catastrophe of microtubules. PloS One 7, e30738.

Gard D, Becker BE, Josh Romney S (2004). MAPping the eukaryotic tree of life: structure, function, and evolution of the MAP215/Dis1 family of microtubule-associated proteins. Int Rev Cytol 239, 179–272.
Gard D, Kirschner M (1987). A microtubule-associated protein from *Xenopus* eggs that specifically promotes assembly at the plus-end. J Cell Biol 105, 2203–2215.
Gell C, Friel CT, Borgonovo B, Drechsel DN, Hyman AA, Howard J (2011). Purification of tubulin from porcine brain. Methods Mol Biol 777, 15–28.
Gorman DS, Levine RP (1965). Cytochrome f and plastocyanin: their sequence in the photosynthetic electron transport chain of *Chlamydomonas reinhardtii*. Proc Natl Acad Sci USA 54, 1665–1669.
Hiller G, Weber K (1978). Radioimmunoassay for tubulin: a quantitative comparison of the tubulin content of different established tissue culture cells and tissues. Cell 14, 795–804.
Howard J, Hyman A (2003). Dynamics and mechanics of the microtubule plus end. Nature 422, 753–758.
Howard J, Hyman A (2007). Microtubule polymerases and depolymerases. Curr Opin Cell Biol 19, 31–35.
Hyman A, Drechsel D, Kellogg D, Salser S, Sawin K, Steffen P, Wordeman L, Mitchison T (1991). Preparation of modified tubulins. Methods Enzymol 196, 478–485.
Janke C, Bulinski JC (2011). Post-translational regulation of the microtubule cytoskeleton: mechanisms and functions. Nat Rev. Mol Cell Biol 12, 773–786.
Johnson V, Ayaz P, Huddleston P, Rice LM (2011). Design, overexpression, and purification of polymerization-blocked yeast alphabeta-tubulin mutants. Biochemistry 50, 8636–8644.
Junqueira M, Spirin V, Santana Balbuena T, Waridel P, Surendranath V, Kryukov G, Adzhubei I, Thomas H, Sunyaev S, Shevchenko A (2008). Separating the wheat from the chaff: unbiased filtering of background tandem mass spectra improves protein identification. J Proteome Res 7, 3382–3395.
Karkhoff-Schweizer R, Knull HR (1987). Demonstration of tubulin-glycolytic enzyme interactions using a novel electrophoretic approach. Biochem Biophys Res Commun 146, 827–831.
Kilmartin JV (1981). Purification of yeast tubulin by self-assembly in vitro. Biochemistry 20, 3629–3633.
Kirkpatrick JB, Hyams L, Thomas VL, Howley PM (1970). Purification of intact microtubules from brain. J Cell Biol 47, 384–394.
Kuriyama R (1976). In vitro polymerization of flagellar and ciliary outer fiber tubulin into microtubules. J Biochem 80, 153–165.
Luduena RF (1998). Multiple forms of tubulin: different gene products and covalent modifications. Int Rev Cytol 178, 207–275.
Mandelkow E, Mandelkow EM (1995). Microtubules and microtubule-associated proteins. Curr Opin Cell Biol 7, 72–81.
McIntosh JR, Pfarr CM (1991). Mitotic motors. J Cell Biol 115, 577–585.
Murphy DB, Borisy GG (1975). Association of high-molecular-weight proteins with microtubules and their role in microtubule assembly in vitro. Proc Natl Acad Sci USA 72, 2696–2700.
Murray AW (1991). Cell cycle extracts. Methods Cell Biol 36, 581–605.
Newton CN, DeLuca JG, Himes RH, Miller HP, Jordan MA, Wilson L (2002). Intrinsically slow dynamic instability of HeLa cell microtubules in vitro. J Biol Chem 277, 42456–42462.
Panda D, Miller HP, Banerjee A, Luduena RF, Wilson L (1994). Microtubule dynamics in vitro are regulated by the tubulin isotype composition. Proc Natl Acad Sci USA 91, 11358–11362.
Ran F, Bali M, Michels CA (2008). Hsp90/Hsp70 chaperone machine regulation of the Saccharomyces MAL-activator as determined in vivo using noninducible and constitutive mutant alleles. Genetics 179, 331–343.
Schiff PB, Fant J, Horwitz SB (1979). Promotion of microtubule assembly in vitro by Taxol. Nature 277, 665–667.
Schneider CA, Rasband WS, Eliceiri KW (2012). NIH Image to ImageJ: 25 years of image analysis. Nat Methods 9, 671–675.
Silflow CD, Sun X, Haas NA, Foley JW, Lefebvre PA (2011). The Hsp70 and Hsp40 chaperones influence microtubule stability in *Chlamydomonas*. Genetics 189, 1249–1260.
Snyder JA, McIntosh JR (1976). Biochemistry and physiology of microtubules. Annu Rev Biochem 45, 699–720.
Sorger PK, Ammerer G, Shore D (1988). Identification and Purification of Sequence-Specific DNA-Binding Proteins. Protein Function; a Practical Approach, Oxford: IRL Press.
Stiernagle T (2006). Maintenance of *C. elegans*. The *C. elegans* Research Community WormBook. Available at: www.wormbook.org/chapters/www_strainmaintain/strainmaintain.html (accessed 18 August 2011).
Studier FW (2005). Protein production by auto-induction in high density shaking cultures. Protein Expr Purif 41, 207–234.
Suprenant KA, Rebhun LI (1984). Purification and characterization of oocyte cytoplasmic tubulin and meiotic spindle tubulin of the surf clam *Spisula solidissima*. J Cell Biol 98, 253–266.
Varga V, Helenius J, Tanaka K, Hyman AA, Tanaka TU, Howard J (2006). Yeast kinesin-8 depolymerizes microtubules in a length-dependent manner. Nat Cell Biol 8, 957–962.
Villasante A, Wang D, Dobner P, Dolph P, Lewis SA, Cowan NJ (1986). Six mouse alpha-tubulin mRNAs encode five distinct isotypes: testis-specific expression of two sister genes. Mol Cell Biol 6, 2409–2419.
Weingarten MD, Lockwood AH, Hwo SY, Kirschner MW (1975). A protein factor essential for microtubule assembly. Proc Natl Acad Sci USA 72, 1858–1862.
Weis F, Moullintraffort L, Heichette C, Chretien D, Garnier C (2010). The 90-kDa heat shock protein Hsp90 protects tubulin against thermal denaturation. J Biol Chem 285, 9525–9534.
Weisenberg RC (1972). Microtubule formation in vitro in solutions containing low calcium concentrations. Science 177, 1104–1105.
Widlund PO, Stear JH, Pozniakovsky A, Zanic M, Reber S, Brouhard GJ, Hyman AA, Howard J (2011). XMAP215 polymerase activity is built by combining multiple tubulin-binding TOG domains and a basic lattice-binding region. Proc Natl Acad Sci USA 108, 2741–2746.
Witman GB (1986). Isolation of *Chlamydomonas* flagella and flagellar axonemes. Methods Enzymol 134, 280–290.